Performance Evaluation of a Complete Lagrangian KTGF Approach for Dilute Granular Flow Modelling

Schalk Cloete[1], Shahriar Amini[2*] & Stein Tore Johansen[2]

1) Department of Energy and Process Technology, NTNU, Trondheim, Norway.

2) Flow Technology Group, Department of Process Technology, SINTEF Materials and Chemistry, Trondheim, Norway.

*Corresponding author. Email: shahriar.amini@sintef.no

Address: SINTEF Materials and Chemistry, Richard Birkelands Vei 3, 7034 Trondheim, Norway, Phone: +47 46639721

Keywords: Kinetic theory of granular flows; Lagrangian; Dense discrete phase model; Clusters.

1. Abstract

Finely resolved gas-solid flow simulations were carried out using an improved Lagrangian method known as the dense discrete phase model (DDPM). The DDPM differs from the traditional Eulerian two fluid model (TFM) approach in that the solids phase is treated as discrete parcels of particles and not as a continuum. This method of particle tracking has several important fundamental advantages over standard Eulerian multifluid approaches including much improved grid independence behaviour and easy inclusion of particle size distributions. Similarly to the TFM, particle collisions and uncorrelated translations are not simulated directly and still need to be modelled by means of the kinetic theory of granular flows (KTGF). This work presents two important improvements to the present state of development of the DDPM: the granular temperature was transported and the additional particle force due to the modelled granular shear stresses was included. The complete model compared well to control simulations carried out using the well-established TFM approach. The impact of the two modelling improvements was also investigated to find large effects, especially with regards to the granular temperature fields. Negligence of granular temperature transport reduced the total amount of granular temperature by a factor of fifteen, while negligence of the shear force resulted in a factor of three increase. It could therefore be concluded that the model improvements are indeed necessary to correctly capture the physics in the dilute riser flows simulated in the present study.

2. Introduction

The kinetic theory of granular flows (KTGF) [1-3] is currently a well established method for modelling granular flows. It has been validated to give adequate representations of the complex flows occurring in bubbling fluidized beds [4] and risers [5]. Traditionally, the KTGF has been applied within an Eulerian-Eulerian multifluid framework, popularly known as the two fluid model (TFM). Within this methodology, the granular phase is represented as a continuum on the assumption that the granular particles are small enough to be adequately simulated as a fluid. Special closure laws from the KTGF are then used to ensure that transport phenomena due to particle collision and translation within this granular fluid are captured correctly.

On the other hand, it is also possible to simulate each individual particle as a separate entity in an Eulerian-Lagrangian framework. This approach, known as the discrete element method (DEM), has also been successfully used to capture dilute granular flows [6, 7]. Here, the particles are tracked individually according to Newton's Laws of motion with particle collisions being simulated directly. Closures from the KTGF are not required in these simulations, but limits in computational capacities severely restrict the size of the system that can be simulated. This approach can therefore only be employed in small scale, fundamental investigations.

The modelling methodology which is the topic of this study takes the middle ground between the TFM and the DEM. In essence, it can be described as an Eulerian-Eulerian-Lagrangian method where the gas phase transport is solved on a fixed Eulerian grid while the particles are tracked in a Lagrangian fashion, but also represented on the Eulerian grid below. This methodology, henceforth called the dense discrete phase model (DDPM) [8], differs from the DEM in that particles are not tracked individually, but rather grouped together in parcels. Each parcel could contain thousands of individual particles, making the DDPM applicable to much larger systems than the DEM. These parcels of particles are nothing more than points of information travelling though the domain. They do not occupy physical space and cannot interact directly. Therefore, the volume fraction of the particulate phase is captured by interpolating the volume fraction that would be occupied by all particles in a cell onto the underlying Eulerian grid and particle collisions and uncorrelated translations are modelled by means of the KTGF.

The DDPM is thus also a KTGF approach, but differs in the way in which the particle phase is transported. This Lagrangian tracking employed by the DDPM has several distinct advantages over the TFM:

- The continuum assumption is dropped. Where the TFM can be argued to give a granular field which is too smooth, that offered by the DDPM can be seen as being too discrete (a large number of particles can be represented by a single point). The impact of these respective assumptions has not been quantified as of yet. Thus far, however, the largest advantage that

has emerged from tracking particle parcels in a Lagrangian way is that there is no numerical diffusion of the particle volume fraction [9]. This will be discussed in more detail later in this introduction.

- A particle size distribution is easily included. The Lagrangian particle tracking framework is much more conducive to including a wide range of particle sizes than the Eulerian framework. The particle size of a Lagrangian parcel will be inherently transported with the particle throughout the domain, whereas only a single averaged particle size can be accommodated in each Eulerian phase. Every new particle size included in the TFM therefore has to be represented as a separate phase adding another set of transport equations to be solved.
- Wall interactions can be simulated directly since the collision between a particle parcel and the wall is simulated directly. This more fundamental approach could reduce the substantial uncertainty involved in wall interactions with the TFM.
- The phenomenon of 'delta shocks' [10] occurring in the TFM is inherently avoided with the DDPM. This effect is observed when two dilute jets of particles are crossing. In reality, since the jets are dilute, they should cross with very little interaction. In the TFM, however, the opposite momentum fluxes entering the point of intersection are averaged, resulting in an unphysical merging of the two streams. When using the DDPM, the momentum of each particle parcel is a property of the particle and will only get altered by the modelled particle-particle interaction when crossing, thus resulting in realistic physical behaviour.

When considering these advantages, the DDPM approach merits some closer investigation as an alternative to the TFM for application to larger granular systems. The DDPM is still a very young model and none of the aforementioned advantages has been properly quantified as of yet. Thus far, the grid independence advantage offered by conducting simulations in the absence of numerical diffusion is seen as the biggest advantage offered by this approach. The improved grid independence behaviour resulted in simulation times up to 10 times shorter than that achieved by the TFM in a relatively dense riser system [9] and has been proven to be even greater in dense bubbling fluidized bed systems [11]. Fluidized bed simulations are inherently transient and require fine meshes to capture the distinct meso-scale structures (bubbles and clusters) formed in these systems. They are therefore very computationally expensive and an order of magnitude reduction in simulation time is a very important advantage.

Due to the novelty of this approach, only limited platforms are available on which to conduct simulations. A code designed for industrial use is available in the form of Barracuda® from CPFD Software LLC, but is not suitable for research purposes since no access to the code is possible. ANSYS FLUENT has included the DDPM in its release 12, allowing much better access to the code by means of

user defined functions (UDF's). This platform is therefore preferred. The improved DDPM investigated in this study is quite close to the Particle in Cell method as presented by Snider [12]. One difference lies in the smoothing function which is simplified in this work, but the most important difference is the Lagrangian transport of the granular temperature from which granular stresses due to collisions and streaming are computed and included in the particle equation of motion.

Two important shortcomings of the present form of the DDPM in FLUENT will be addressed in this paper:

- The transport of granular temperature is not included.
- Only the normal KTGF stresses are included in the modelled particle-particle interaction force.

Once these shortcomings are addressed, the DDPM would include the same physics as the TFM and a proper comparison can be made. This work will focus on presenting the new improvements in DDPM and validating the newly included model alterations against the TFM.

3. Nomenclature

Regular symbols

C_D	Drag coefficient
d	Diameter (m)
$\vec{F}$	Force vector per unit mass (m/s^2)
$\vec{g}$	Gravity vector (m/s^2)
$\overline{I}$	Identity tensor
K_{gs}	Interphase momentum exchange coefficient (kg/(m^{3}s))
k_Θ	Diffusion coefficient (kg/(m.s))
p	Pressure (Pa)
Re	Reynolds number
t	Time (s)

Greek symbols

α	Volume fraction
ϕ_{gs}	Interphase energy exchange rate (W/m^3)
γ_Θ	Energy dissipation rate (W/m^3)

λ Bulk viscosity (kg/(m.s))

μ Shear viscosity (kg/(m.s))

Θ Granular temperature (m^2/s^2)

ρ Density (kg/m^3)

$\bar{\bar{\tau}}$ Stress-strain tensor ($kg/(m.s^2)$)

$\vec{\upsilon}$ Velocity vector (m/s)

∇ Gradient/Divergence (1/m)

Sub/Superscripts

g Gas

p Particle

s Solids

T Transpose

4. Simulations

4.1 Model equations

Model equations for the TFM have been well documented in the literature. The exact set of equations employed in the present study is summarized in Cloete *et al.* [13].

A full dissemination of the DDPM equations will be presented. The DDPM is based on the standard discrete phase modelling (DPM) approach where parcels of particles are tracked through the domain in a Lagrangian framework according to Newton's laws of motion. In its standard form, the DPM does not account for the volume fraction of the discrete phase particles. The DDPM formulation [8] overcomes this limitation by solving a set of conservation equations for multiple phases as is done in a Eulerian multifluid approach.

$$\frac{\partial}{\partial t}\left(\alpha_g \rho_g\right)+\nabla\cdot\left(\alpha_g \rho_g \vec{\upsilon}_g\right)=0 \qquad (1)$$

$$\frac{\partial}{\partial t}\left(\alpha_s \rho_s\right)+\nabla\cdot\left(\alpha_s \rho_s \vec{\upsilon}_s\right)=0 \qquad (2)$$

$$\frac{\partial}{\partial t}\left(\alpha_g \rho_g \vec{\upsilon}_g\right)+\nabla\cdot\left(\alpha_g \rho_g \vec{\upsilon}_g \vec{\upsilon}_g\right)=-\alpha_g \nabla p+\nabla\cdot\bar{\bar{\tau}}_g+\alpha_g \rho_g \vec{g}+K_{sg}\left(\vec{\upsilon}_s-\vec{\upsilon}_g\right) \qquad (3)$$

$$\frac{\partial}{\partial t}\left(\alpha_s \rho_s \vec{\upsilon}_s\right) + \nabla \cdot \left(\alpha_s \rho_s \vec{\upsilon}_s \vec{\upsilon}_s\right) = -\alpha_s \nabla p + \nabla \cdot \bar{\bar{\tau}}_s + \alpha_s \rho_s \vec{g} + K_{gs}\left(\vec{\upsilon}_g - \vec{\upsilon}_s\right) \quad (4)$$

The conservation equations are not solved for the solids phase, but the appropriate volume fraction or velocity values are taken directly from the particle field. This is illustrated graphically in Figure 1. Only the volume fraction field will be used in subsequent figures in order to allow for easy comparison with results from the TFM.

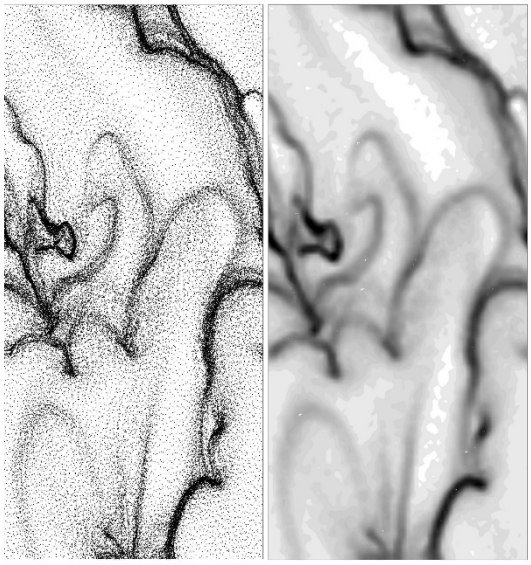

Figure 1: The dispersed phase volume fraction field (right) derived form the particle tracks (left).

The particle equation of motion is solved for each particle in the form:

$$\frac{d\vec{\upsilon}_p}{dt} = F_D\left(\vec{\upsilon} - \vec{\upsilon}_p\right) + \frac{\vec{g}\left(\rho_p - \rho\right)}{\rho_p} + \vec{F}_{KTGF} \quad (5)$$

Equation (5) is standard for the DPM where the acceleration of each particle is calculated from the sum of the force contributions due to inter-phase drag and gravity. An additional term is included to simulate effects due to particle collisions and translations which arise from the KTGF. The drag force is calculated as follows:

$$F_D = \frac{18\mu}{\rho_p d_p^2}\frac{C_D \,\mathrm{Re}_p}{24} \quad (6)$$

Where the drag coefficient is calculated according to Wen and Yu [14] (Table 1) and is adjusted with a factor of $\alpha_g^{-3.65}$ to account for the hindered settling effect:

$$C_D = \frac{24}{\alpha_g \,\mathrm{Re}_p}\left[1 + 0.15\left(\alpha_g \,\mathrm{Re}_p\right)^{0.687}\right]\alpha_g^{-3.65} \quad (7)$$

The KTGF force results from the stresses generated due to particle collisions and translations and is modelled from the solids phase stress tensor:

$$\vec{F}_{KTGF} = \frac{-1}{\alpha_p \rho_p} \nabla \bar{\bar{\tau}}_s \qquad (8)$$

Where the stress tensor includes the normal and shear viscous stresses as well as the normal pressure:

$$\bar{\bar{\tau}}_s = -p_s \bar{\bar{I}} + 2\mu_s \bar{\bar{S}} + \left(\lambda_s - \frac{2}{3}\mu_s \right) \cdot \nabla \vec{\upsilon}_s \bar{\bar{I}} \qquad (9)$$

Due to implementation difficulties, only the solids pressure (first term in equation (9)) is presently included in ANSYS FLUENT. The shear and normal viscous stresses (second and third terms) were included in the present study to check the validity of this simplifying assumption. Shear stresses in a gas-solid system result from collisions and uncorrelated particle motions dispersing momentum in all directions. This stress contribution is expected to have a large effect in regions of high granular temperature.

The solids pressure [1], shear viscosity [2] and bulk viscosity [1] used in equation (9) is calculated from the KTGF and depends on the conservation of the kinetic energy contained in uncorrelated particle motions. This quantity, popularly termed the granular temperature comes from the kinetic theory of gasses where the temperature is used to express the energy contained in random motions of gas molecules. In conservative form it is written as follows:

$$\frac{3}{2}\left[\frac{\partial}{\partial t}\left(\alpha_s \rho_s \Theta \right) + \nabla \cdot \left(\alpha_s \rho_s \vec{\upsilon}_s \Theta \right) \right] = \bar{\bar{\tau}}_s : \nabla \vec{\upsilon}_s + \nabla \cdot \left(k_\Theta \nabla \Theta \right) - \gamma_\Theta + \phi_{gs} \qquad (10)$$

From left to right equation (10) includes a transient term, a convection term, a generation term due to solids stresses, a diffusion term [2], a sink term due to inelastic particle collisions [2] and a sink term due to inter-phase damping [2]. The formulation of the various closure laws is given in Table 1.

Table 1: Closure formulations used in this study.

Drag coefficient [14]	$C_D = \frac{24}{\alpha_g \mathrm{Re}_s}\left[1+0.15\left(\alpha_g \mathrm{Re}_s\right)^{0.687}\right]$
Solids pressure [1]	$p_s = \alpha_s \rho_s \Theta_s + 2\rho_s\left(1-e_{ss}\right)\alpha_s^2 g_{0,ss}\Theta_s$
Shear viscosity [2]	$\mu_s = \mu_{s,col} + \mu_{s,kin}$
	$\mu_{s,col} = \frac{4}{5}\alpha_s \rho_s d_s g_{0,ss}\left(1+e_{ss}\right)\left(\frac{\Theta_s}{\pi}\right)^{1/2}$
	$\mu_{s,kin} = \frac{10\rho_s d_s\sqrt{\Theta_s \pi}}{96\alpha_s\left(1+e_{ss}\right)g_{0,ss}}\left[1+\frac{4}{5}\alpha_s g_{0,ss}\left(1+e_{ss}\right)\right]^2$
Bulk viscosity [1]	$\lambda_s = \frac{4}{3}\alpha_s \rho_s d_s g_{0,ss}\left(1+e_{ss}\right)\left(\frac{\Theta_s}{\pi}\right)^{1/2}$
Granular temperature diffusion coefficient [2]	$k_{\Theta_s} = \frac{150\rho_s d_s\sqrt{\Theta_s\pi}}{384\left(1+e_{ss}\right)g_{0,ss}}\left[1+\frac{6}{5}\alpha_s g_{0,ss}\left(1+e_{ss}\right)\right]^2 + 2\rho_s\alpha_s^2 d_s\left(1+e_{ss}\right)g_{0,ss}\sqrt{\frac{\Theta_s}{\pi}}$
Collisional dissipation [2]	$\gamma_{\Theta_s} = \frac{12\left(1-e_{ss}^2\right)g_{0,ss}}{d_s\sqrt{\pi}}\rho_s\alpha_s^2\Theta_s^{3/2}$
Inter-phase damping [2]	$\phi_{gs} = -3K_{gs}\Theta_s$

If equation (10) is to be solved as a partial differential equation, the convective granular temperature flux has to be calculated from the velocity field passed down from the Lagrangian particle tracks. This cannot be made to run stably at present, however, and ANSYS FLUENT recommends that equation (10) only be solved in its algebraic form by neglecting the convection and diffusion terms. An algebraic solution of the granular temperature equation could be a reasonable approximation in dense, slow moving beds where the local generation and dissipation of granular energy will strongly outweigh the convective and diffusive fluxes crossing the cell boundaries, but becomes invalid in more dilute, fast moving systems.

In order to address this challenge, the granular temperature was also expressed in Lagrangian form so that granular temperature would be automatically convected by the particle parcels. This does not imply that the granular temperature is a property of single particles, but only that this statistical particle cloud

property is now transported in a manner which is less numerically diffusive and more numerically stable. The Lagrangian granular temperature equation is written as follows:

$$\frac{3}{2}\alpha_s\rho_s\frac{d\Theta}{dt} = \overline{\overline{\tau}}_s : \nabla\vec{\upsilon}_s + \nabla\cdot\left(k_\Theta\nabla\Theta\right) - \gamma_s + \phi_{gs} \qquad (11)$$

Equation (11) was solved algebraically at every DPM iteration using the present granular temperature field to calculate the diffusion of granular temperature. The granular temperature on the Eulerian grid was taken as a mass-weighted average of the granular temperature on all parcels residing inside a particular cell. Using this methodology, the stability problems created by the interpolated granular temperature fluxes were successfully resolved and the full transport of granular temperature could be solved.

4.2 Geometry and boundary conditions

As a first stage of testing, flow was solved on a fully periodic 2D plane in order to avoid the uncertainty that stems from wall-interactions. After some initial testing a domain of 10 cm in width and 20 cm in height was chosen. These dimensions were found to be sufficiently large to prevent a single cluster from spanning the entire domain, thereby creating the unphysical situation of an infinitely periodically repeated cluster.

The domain was meshed with square, structured cells, 15 particle diameters in height and width. This cell size was proven to give sufficiently grid independent solutions with the TFM [15].

The pressure drop over the periodic section was continuously adjusted in order to maintain the superficial velocity through the section at 5 m/s.

4.3 Physical properties

Standard air at room temperature was used as the carrier phase. The particle phase was specified to consist of typical Geldart A particles, 100 µm in diameter with a density of 1500 kg/m^3.

4.4 Start-up procedure

Simulations were started with a uniform distribution of solids at a volume fraction determined by the specific experiment under consideration. For the DDPM, a single injection of particles on all the cell edges within the domain was done at the beginning of the simulation such that each cell would, on average, contain 10 particle parcels. A small square of high granular temperature was subsequently patched in to create an initial disturbance and speed up the breakdown of the flow into clusters. The solids flux through the domain was continuously monitored to establish when a quasi-steady state was achieved and data collection was subsequently commenced.

4.5 Performance variables

Three main performance variables were collected. All three these variables were time averaged for a minimum of 15 seconds once the quasi-steady state has been achieved. The three time average values extracted included the following.

- Total flux over the geometry. This measure would indicate the degree of momentum coupling between the two phases.
- Spatial standard deviation of the volume fraction field on the geometry. A well segregated flow with distinct clusters would register large amounts of spatial volume fraction variation within the domain. This value was therefore used as an indication of the degree of cluster formation resolved.
- Mass averaged granular temperature. This measure would indicate the amount of kinetic energy contained in the random particle motions modelled by the KTGF and would therefore be a direct measure of the degree to which the KTGF influences the simulation.

4.6 Solver settings

The commercial flow solver ANSYS Fluent 12.1 was used to complete the calculations. The phase coupled SIMPLE algorithm was used for pressure-velocity coupling, while all other variables were discretized using the QUICK scheme.

Second order temporal discretization was used for the TFM in accordance with the findings of Cloete *et al.* [15]. These findings were confirmed for this study by running a simulation both with first and second order implicit timestepping. The results are given in Table 1.

Table 2: Results from the DDPM and TFM for first and second order timestepping.

Model	Solids flux (kg/m^{2}s)	Standard deviation	Granular temperature (m^2/s^2)
TFM 1st order	61.0	0.0142	0.0106
TFM 2nd order	61.0	0.0160	0.0155
DDPM 1st order	62.6	0.0145	0.0128
DDPM 2nd order	63.1	0.0147	0.0127

From the performance measures in Table 1, it can be seen that there are substantial differences between the solutions returned with the TFM for all the performance variables except for the averaged flux. Generally, the use of first order timestepping resulted in much elongated clusters often stretching over the entire length of the periodic domain (see Figure 2). Clusters were also less well resolved as can be seen from the standard deviation statistic in Table 1, confirming a significant increase in numerical diffusion under lower order temporal discretization. The constant value of the flux can be explained by

considering two opposing error inducing effects: a decrease in flux due to the elongated clusters which are much more streamlined in the flow direction and an increase in flux due to the poorer cluster resolution an the subsequent increased momentum coupling between phases. In this particular case, these two opposing effects seem to cancel each other out exactly.

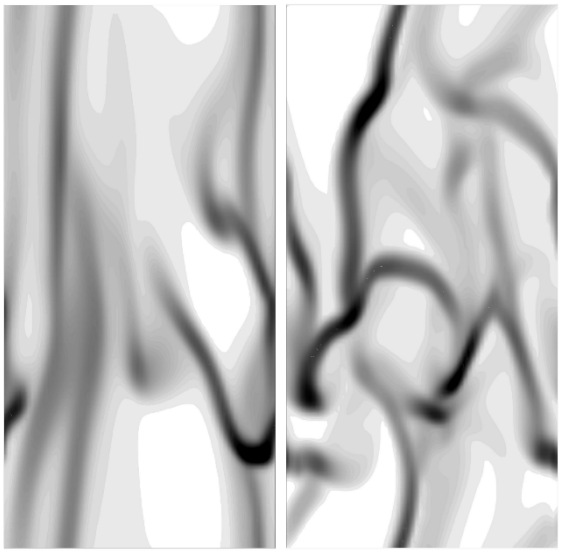

Figure 2: Clusters formed by the TFM when 1st order timestepping (left) and 2nd order timestepping (right) is used.

The DDPM with the additional model enhancements could not be made to run stably when 2nd order timestepping was used, but fortunately, this does not have an equally significant effect on the performance of the model (Table 1). The simulation with 2nd order timestepping shown in Table 1 was carried out with very conservative multigrid settings and very small timesteps, making the model about 5 times slower when 2nd order timestepping is used. The primary reason for the similar performance between 1st and 2nd order timestepping with the DDPM is simply that this Lagrangian approach is not subject to numerical diffusion. Therefore, the extra numerical diffusion of the volume fraction field caused by 1st order temporal discretization is not applicable to simulations carried out using the DDPM and there is nothing to be gained by using a higher order scheme.

4.7 Variable smoothing

An additional step had to be completed in order to ensure correct behaviour from the DDPM. Due to the discrete nature of the DDPM, the variable fields in more dilute flow regions can become very discontinuous. For example, one cell could contain two parcels, while its neighbour contains no parcels, thereby creating a sudden discontinuity in the volume fraction field. The KTGF often requires the calculation of gradients and is therefore severely affected by these discontinuities.

A smoothing algorithm was therefore implemented in the present work in which the averaging of particle variables onto the underlying Eulerian grid would be done over a minimum number of particles.

This was done by expanding the area over which the averaging was done to include neighbouring cells if a particular cell contained less than a specified number of parcels. For example, if it is specified that averaging has to be done over at least 10 parcels and the parcel-in-cell situation shown in Figure 3 is presented, the following procedure is followed:

- The number of parcels lacking in the averaging procedure is calculated – 8 in this case.
- These 8 particles will therefore have to be included by extending the averaging area to the neighbouring cells. In this case, the four neighbouring cells contain an additional 16 particles.
- The new cell value is then calculated by averaging over the cell and its neighbours, with the contribution from the neighbouring cells being weighted according to how many additional parcels are required. In this case, the weighting of the neighbouring cells would be 8/16 = 0.5 since 8 more parcels are needed and 16 are available.
- The smoothed number of parcels for the situation in Figure 3 would therefore be $\left(2+0.5\left(3+5+4+4\right)\right)\Big/\left(1+0.5\times 4\right)=3.33$.
- If more parcels are required than is available from the neighbouring cells, a maximum weighing of 1 is used in the calculations.

This smoothing was employed on the volume fraction field, the velocity field and the granular temperature field.

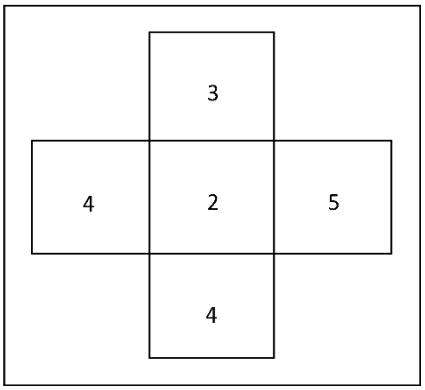

Figure 3: A central cell with four surrounding neighbours each housing a specified number of particle parcels.

This smoothing strategy applied to the solids volume fraction field is displayed in Figure 4. Incidentally, even large errors in the gradients computed in the dilute regions were tested to not have a very large influence on the overall system performance since the error only affects a small portion of the solids inside the domain. The smoothing will therefore not cause substantial increases in overall model accuracy, but it does offer a substantial improvement in model stability.

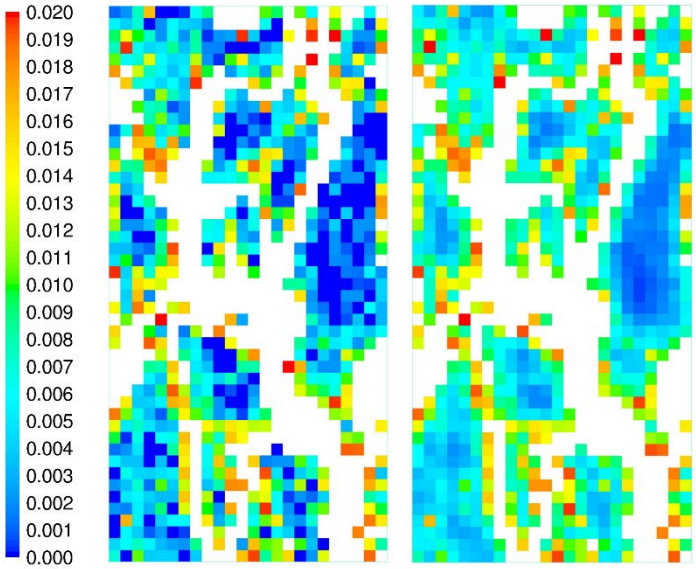

Figure 4: The particle volume fraction field before (left) and after smoothing. Cells with a volume fraction exceeding 0.02 are coloured white.

5. Results and discussion

Two sets of simulation experiments were performed. The first was a validation study of the upgraded DDPM against the TFM over a range of overall volume fractions and the second investigated the impact of the improvements made to the DDPM formulation.

5.1 Validation study

Comparisons were made between the DDPM and the TFM for five different volume fractions spanning a range between 0.01 and 0.05. Model results are shown in Table 2.

Table 3: Performance of the DDPM and the TFM over a range of volume fractions.

Volume fraction	Solids flux (kg/m^{2}s)			Standard deviation of solids volume fraction			Granular temperature (m^2/s^2)		
	DDPM	TFM	% diff	DDPM	TFM	% diff	DDPM	TFM	% diff
0.01	63.0	61.0	3.23	0.0145	0.0160	-9.84	0.0128	0.0155	-19.08
0.02	124.0	118.7	4.37	0.0289	0.0324	-11.42	0.0095	0.0105	-10.00
0.03	184.8	176.5	4.59	0.0445	0.0484	-8.40	0.0076	0.0081	-6.37
0.04	248.8	237.3	4.73	0.0589	0.0634	-7.36	0.0057	0.0061	-6.78
0.05	316.9	301.5	4.98	0.0739	0.0774	-4.63	0.0042	0.0047	-11.24

Table 2 shows a close agreement between results produced by the TFM and the DDPM throughout the comparison, indicating that the same physics is being captured by both modelling methodologies. Results are not identical, however. The solids flux predicted by the TFM is consistently lower than that

predicted by the DDPM, while this trend is opposite for the standard deviation. These two quantities are related in that a more clustered flow would generally result in greater inter-phase slip (here expressed as a decreased solids flux). It is therefore to be expected that the lower standard deviation returned by the DDPM would result in higher fluxes.

The phenomenon of delta shocks [10] (discussed in the introduction) is seen as the primary reason for the somewhat higher degree of clustering predicted by the TFM. It is also interesting to note that the difference between the standard deviations returned by the DDPM and the TFM reduces from about 10% at the lowest volume fraction to about 5% at the highest volume fraction. Under the assumption that the DDPM is the more accurate representation, it can be concluded that the degree to which clustering is over-predicted by the TFM decreases with an increase in volume fraction. This is to be expected since the delta shock phenomenon will be a more physical representation of reality if denser particle streams attempt to cross. The degree of clustering predicted by the DDPM and TFM should therefore approach the same limit as the solids loading of the system is increased.

In contrast to this trend, however, the difference in the solids flux predicted by the two models increases slightly from 3% to 5% with the overall solids loading. This is a clear indication that the resolution of clusters plays a less significant role in dilute systems [5] where a 10% increase in clustering only resulted in a 3% decrease of the flux. Here, the modelled drag on a particle is more important and the correct modelling of cluster formation is not as crucial. In denser systems, however, clusters become very heavy and start to dominate the inter-phase momentum transfer. For the densest system investigated here, a 5% increase in the clustering resulted in a 5% decrease in the flux. This is a further indication that the correct prediction of clustering becomes increasingly important as the solids mass loading is increased.

The ±10% difference between the granular temperature predictions of the two models is also related to the difference in cluster resolution. The denser clusters resolved by the TFM are heavier and fall more readily against the fluidizing air stream. This creates greater velocity gradients around the cluster and leads to a greater generation of granular temperature due to solids stresses. This was confirmed by monitoring the maximum and minimum vertical gas phase velocities in the domain for the most dilute case. The average maximum and minimum velocities in the TFM case were 7.39 and 2.90 m/s respectively, while those for the DDPM were 7.16 and 3.33 m/s. This confirms that the heavier clusters formed by the TFM create greater velocity segregation in the flow field, leading to larger velocity gradients and greater granular temperature generation.

Representative snapshots of the clusters formed by the two modelling approaches are given in Figure 5.

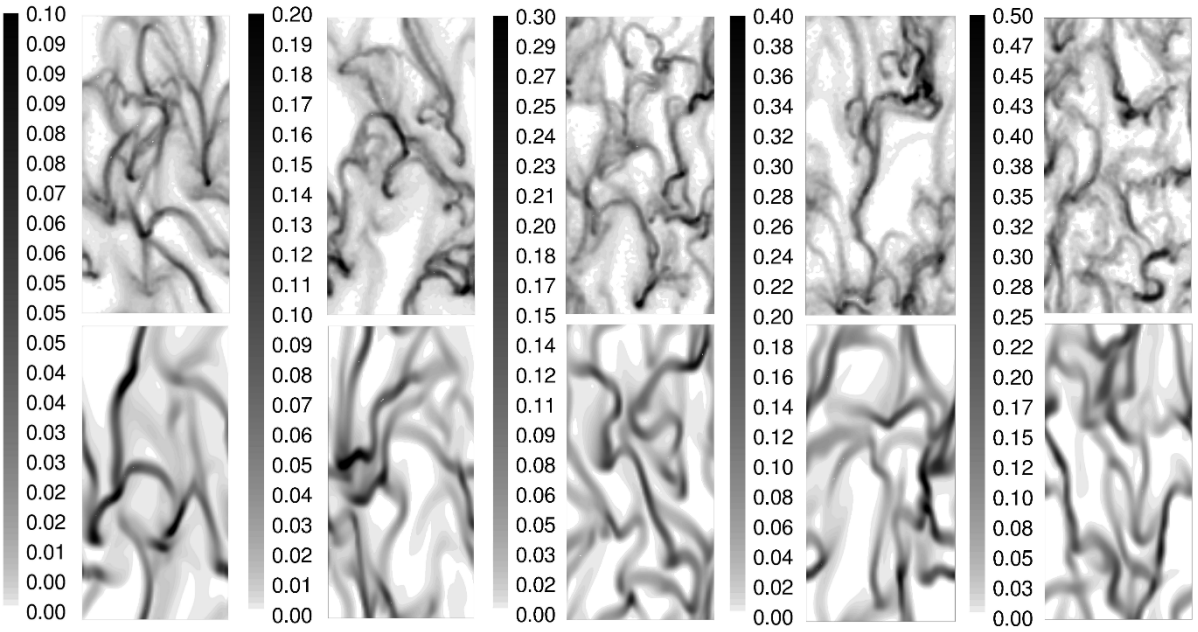

Figure 5: Instantaneous snapshots of particle volume fraction solved by the DPDM and TFM for different volume loadings. The upper row is the DDPM and the bottom row the TFM. Initial volume loading is increased in intervals of 0.01 from 0.01 on the left to 0.05 on the right.

It is immediately evident that that the structures resolved by the DDPM are significantly finer than those of the TFM. A substantially greater degree of flow detail is resolved with the DDPM and, in general, the solution does not appear as unrealistically smooth as is does with the TFM. These effects can be explained by the Lagrangian particle tracking employed by the DDPM. Since the particles are now tracked as discrete parcels and not as a fluid any longer, the particle volume fraction field seems more discrete and particle-like. Additionally, the very important advantage of the DDPM in that the volume fraction field is not subject to numerical diffusion enables more flow details to be solved on any particular grid size. Even though the TFM is considered to give sufficiently grid independent results on this particular grid when measured in terms of time average flow variables, the degree of flow detail resolved still changes if the grid is refined further. This is illustrated in Figure 6.

It is interesting to note that even though substantially greater flow detail is resolved with the DDPM, more substantial volume fraction segregation is predicted by the TFM. This is an additional indication that the formation of delta-shocks has a significant impact on results by increasing the amount of clustering predicted by the TFM.

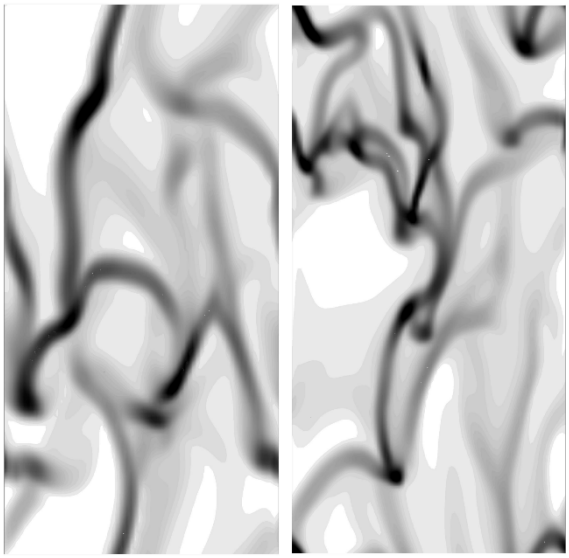

Figure 6: Cluster detail resolved with the TFM on a grid of 15 particle diameters (left) and 11 particle diameters (right).

5.1.1Isolated study on delta-shocks

In order to better understand the delta-shock phenomenon, simulations were performed where two diagonal jets were injected from opposite sides of the domain and allowed to interact. No drag force or gravity was included so as to isolate the interactions between the crossing solids jets. In reality, the solids jets should cross and interact to some degree depending on the solids loading. This is reasonably predicted by the DDPM, but completely misrepresented by the TFM as shown in Figure 7.

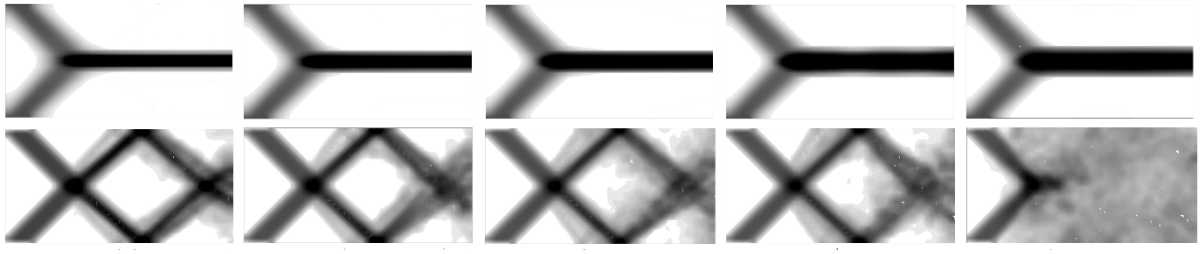

Figure 7: The crossing jet simulation solved for jet volume fractions of 0.05, 0.1, 0.15, 0.2 and 0.25 from left to right. The top and bottom rows show volume fraction contours generated with the TFM and DDPM respectively. The volume fraction range used from left to right is identical to that indicated in Figure 5.

It is clear that the TFM creates one large delta-shock in every case. The positive and negative velocity components meeting at the point of intersection are averaged to zero within the TFM framework. With the DDPM, on the other hand, the jets are allowed to cross with a certain amount of modelled interaction and proceed to bounce off the perfectly elastic walls, causing further interaction between particles approaching and particles leaving the wall. Figure 7 shows that the degree of interaction increases steadily with the solids loading of the jets until a sudden apparent explosion occurs at a jet volume fraction of 0.25. At this point, the crossing jets are dense enough to reach the maximum packing

limit as they cross. The radial distribution function, determining the likelihood of collisions between particles, rapidly increases to infinity in the limit of the maximum packing limit, simulating very strong particle interaction forces in the region of crossing. Due to this very large interaction force, primarily related from the granular pressure, all particles are strongly accelerated away isotropically from the region of crossing as is shown in the bottom plot in Figure 8.

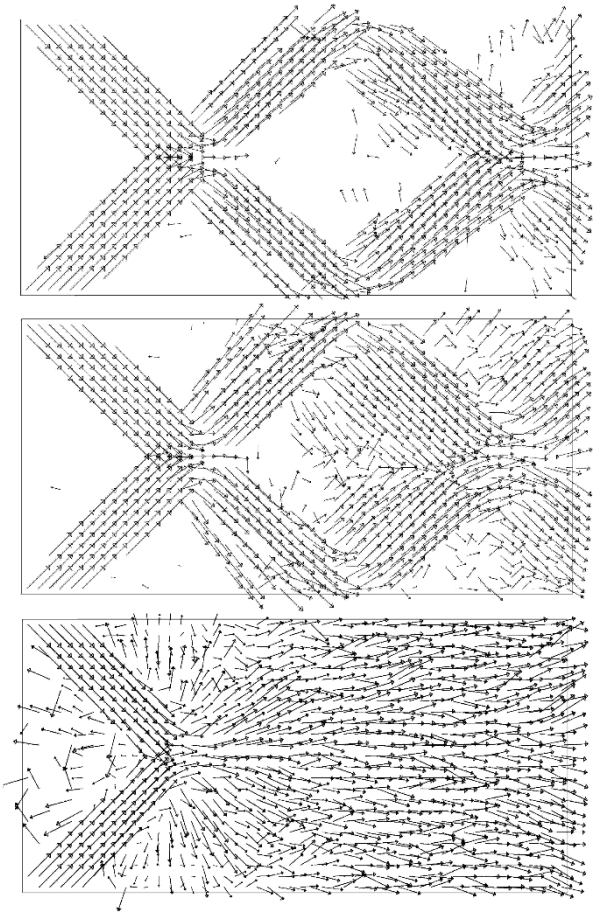

Figure 8: Velocity vectors for the particle phase returned from the DDPM simulations for crossing dilute jets with a volume fraction of 0.05, 0.15 and 0.25 from top to bottom.

Even though the flow situation considered here is an extreme case, it is clear that crossing clusters in a riser flow will also be simulated very differently by the TFM and the DDPM. Clusters simulated by the TFM will merge while clusters simulated by the DDPM will cross with a certain degree of interaction. It can therefore safely be concluded that the higher degree of clustering predicted by the TFM results from the delta-shock phenomenon. If no delta-shocks were present in the TFM, the degree of clustering (standard deviation in Table 2) would be lower than that of the DDPM due to numerical diffusion. The increased amount of numerical diffusion allowed by the TFM in comparison to the DDPM can also be seen in Figure 7 by comparing the volume fraction contours of the jets before crossing. The TFM therefore over-predicts clustering by at least 10% in dilute riser flows. This number is significant albeit not critical.

5.2 Study on the effects of model improvements

The work done in this study was originally motivated when the highly favourable results reported in Cloete *et al.* [9] could not be repeated for more dilute flow scenarios. The aforementioned study showed that the DDPM without the transport of granular temperature or viscous stress contribution could correctly capture relatively dense riser flow. These simulations were subsequently repeated in more dilute flow regimes, but correct predictions could not be attained.

It is therefore reasoned that the model behaved correctly in the dense limit because the majority of clusters were at the maximum packing limit. These clusters would form on the rough walls and grow larger due to their incompressibility at the packing limit until they protrude sufficiently far into the domain to be swept up by the central stream again. When more dilute flow scenarios are simulated, the clusters will not grow at the wall, but only become denser. Additional granular forces, modelled from the granular temperature are then required to define the cluster. When the transport of granular temperature is not included in dilute riser flows, the granular temperature is strongly under-predicted and these forces are weakened accordingly. Clusters are therefore not defined and never get entrained back into the rising gas stream. The result is large negative fluxes next to the walls and unrealistically large strain rates.

Both the improvements employed in the present study are necessary to correct the situation described above. The transport of granular temperature needs to be included in order to increase the granular temperature and help define clusters by concentrating solids in regions of low granular temperature, while the inclusion of the force due to shear stresses is required to prevent unrealistically large strain rates by offering a resistance to strain.

The actual quantitative effect of these improvements is not known at present and will be studied in this section. In order to do this, the most dilute flow scenario (initial solids volume fraction of 0.01) was repeated for two further simulations:

- A simulation in which the granular temperature is transported on the particles, but the particle-particle interaction forces modelled only from the granular pressure. In other words, no viscous force contribution was included.
- A simulation in which no transport of granular temperature is included and the particle-particle interaction forces were also modelled only from the granular pressure. This is the simulation setup which is currently available within ANSYS Fluent 12.1.

Results from these three alternative modelling strategies are presented in Table 3.

Table 4: Results from the DDPM for the three different modelling methodologies.

Model	Solids flux (kg/m^{2}s)	Standard deviation	Granular temperature (m^2/s^2)
No granular temperature transport or viscous shear force	64.3	0.0125	0.0023
No viscous shear force	63.1	0.0137	0.0354
All included	62.6	0.0145	0.0128

Table 3 shows some differences between the output returned by the three modelling methodologies in terms solids flux and standard deviation. The granular temperature performance measure, however, is by far the most affected. Inclusion of the transport of granular temperature caused the total fluctuating energy in the system to increase by a factor of 15. Then, when the viscous shear force was subsequently included, the total fluctuating energy decreased by a factor of 3 again. It is therefore shown that these two model improvements have opposite effects on the modelled granular temperature and combine to cause a factor of five times increase in the granular temperature when both are included.

The very large under-prediction in fluctuating energy within a system where no convection of granular temperature is included was expected. This large reduction is also observed in simulations with the TFM when the granular temperature conservation equation is solved algebraically. Granular temperature generation is the most significant on the face of clusters where high rates of strain occur. It is very important that the energy contained within these uncorrelated particle motions is then transported with the flow back into the more dilute flow regions. The most important dissipation mechanism, that due to inelastic collisions, is very weak in these dilute regions. Therefore, the contributions of local generation and dissipation of granular temperature in any particular dilute cell is significantly lower than the contribution of convection of granular temperature from regions of high strain rate.

When the granular temperature is transported, but particle forces resulting from shear stresses are neglected, there is a substantial increase in the overall granular temperature in the system. The inclusion of such forces will offer a resistance to strain by correctly simulating the diffusive influence of uncorrelated particle fluctuations. When this force is neglected, strain rates inside the system are allowed to become much larger. Strain rates are also the only mechanism by which granular temperature is generated, and these increased strains therefore significantly increase the amount of granular temperature inside the system.

A visual representation of the influence of these models and applications on cluster formation is presented in Figure 9.

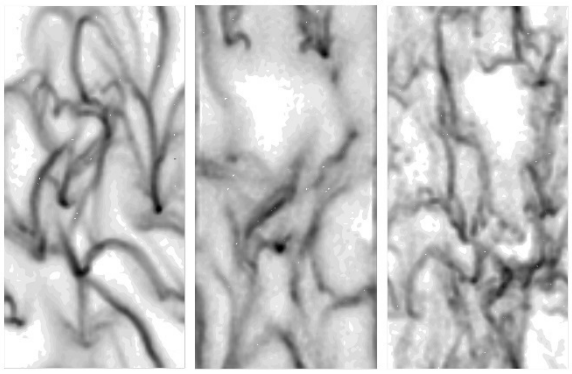

Figure 9: Instantaneous snapshots of particle volume fraction obtained with the full model (left), the negligence of shear forces (middle) and the negligence of granular temperature transport (right).

Clear differences in model behaviour are visible from Figure 9, but it is interesting to note that all three models predict clustering. This is also emphasised by the relatively small difference in the standard deviation statistic given in Table 3. The clustering observed in the model without any granular temperature transport is especially noteworthy in that it proves that clustering can be predicted with virtually no influence from the KTGF. Clusters are therefore almost exclusively formed through wake effects allowing trailing particles to catch up with leading ones, thereby forming a cluster. The inclusion of granular forces does create a much smoother cluster field though, but when the shear forces are neglected, the clusters seem to be degenerating again.

Despite the big differences observed in Figure 9, the solids fluxes predicted by the three modelling approaches are quite similar (Table 3). This is the result of the fully periodic system simulated here not displaying any radial segregation. When walls are included and solids start accumulating next to the walls, the correct modelling of granular stresses will be essential to capture the correct interaction between the core and the annulus. The failure of the DDPM without granular temperature transport can be attributed to the severe under-prediction of these stresses. Future work will evaluate the performance of this full model in a wall bounded system that is more sensitive to granular stress modelling.

6. Conclusions

An improved Lagrangian method for modelling granular flows was developed and tested within a finely resolved fully periodic domain. The dense discrete phase model (DDPM) available within ANSYS Fluent 12.1 was used as the basis for two important improvements: the full transport of granular temperature and the inclusion of granular forces resulting from viscous shear stresses.

The resulting model performed well when compared against the well developed two fluid model (TFM) over a range of solids loadings. A comparison of these results suggested that the formation of delta-shocks (unphysical merging of two crossing dilute particle jets) is the primary reason for the minor

differences in performance between the DDPM and the TFM, causing about 10% more clustering with the TFM. Separate simulations with crossing dilute particle jets confirmed the radically different behaviour of the DDPM and the TFM when two opposing fluxes of particles interact. It was also shown that the DDPM resolved finer details in the volume fraction field than the TFM on a similarly sized grid. This could be attributed to the DDPM not being subject to numerical diffusion of the volume fraction field.

The nature and magnitude of the improvements offered by the modelling enhancements added in this work were also evaluated. It was shown that, when the transport of granular temperature was included, the amount of fluctuating energy in the system increased with a factor of 15. In a dilute system, almost all of the granular temperature is generated in denser regions around the clusters and it is essential that this fluctuating energy be transported to more dilute regions through convection. If not, the granular temperature and subsequent granular stresses will be strongly under-predicted and the model will fail.

When the viscous stresses were subsequently included, the total granular temperature inside the system decreased again by a factor of three. This was a direct result of removing the over-predicted strain rates caused by neglecting shear stresses (essentially simulating a non-viscous flow). A model excluding a viscous contribution to the particle force balance therefore not only neglects the shear stresses, but also substantially over-predicts the normal stresses modelled from the granular temperature.

Subsequent work will evaluate the performance of the DDPM in a wall bounded system where substantial radial volume fraction segregation is present in order to assess its ability to predict real riser flows.

7. Acknowledgement

The authors would like to acknowledge the funding received from the Research Council of Norway which enabled the completion of this work.

8. References

[1] Lun CKK, Savage SB, Jeffrey DJ, Chepurniy N. Kinetic Theories for Granular Flow: Inelastic Particles in Couette Flow and Slightly Inelastic Particles in a General Flow Field. Journal of Fluid Mechanics. 1984;140:223-56.

[2] Gidaspow D, Bezburuah R, Ding J. Hydrodynamics of Circulating Fluidized Beds, Kinetic Theory Approach. *7th Engineering Foundation Conference on Fluidization* 1992:75-82.

[3] Syamlal M, Rogers W, O'Brien TJ. MFIX Documentation: Volume 1, Theory Guide. Springfield: National Technical Information Service 1993.

[4] Taghipour F, Ellis N, Wong C. Experimental and computational study of gas-solid fluidized bed hydrodynamics. Chemical Engineering Science. 2005;60(24):6857-67.

[5] Ellis N, Xu M, Lim CJ, Cloete S, Amini S. Effect of Change in Drag Force in Riser Hydrodynamics - Experimental and Numerical Investigations. Industrial & Engineering Chemistry Research. 2011;In press.

[6] Zhang MH, Chu KW, Wei F, Yu AB. A CFD-DEM study of the cluster behavior in riser and downer reactors. Powder Technology. 2008;184(2):151-65.
[7] Zhao Y, Cheng Y, Wu C, Ding Y, Jin Y. Eulerian-Lagrangian simulation of distinct clustering phenomena and RTDs in riser and downer. Particuology. 2010;8(1):44-50.
[8] Popoff B, Braun M. A Lagrangian Approach to Dense Particulate Flows. *6th International Conference on Multiphase Flow*. Leipzig, Germany 2007.
[9] Cloete S, Johansen ST, Braun M, Popoff B, Amini S. Evaluation of a Lagrangian Discrete Phase Modeling Approach for Resolving Cluster Formation in CFB Risers. 7th International Conference on Multiphase Flow; 2010; Tampa, FL USA; 2010.
[10] Passalacqua A, Fox RO. Multiphase CFD for Gas-Particle Flows: Beyond the Two-Fluid Model. *Seventh International Conference on CFD in the Minerals and Process Industries*. CSIRO, Melbourne, Australia 2009.
[11] Cloete S, Johansen ST, Braun M, Popoff B, Amini S. Evaluation of a Lagrangian Discrete Phase Modelling Approach for Application to Industrial Scale Bubbling Fluidized Beds. 10th International Conference on Circulating Fluidized Bed and Fluidized Bed Technology; 2011; Sunriver, Oregon, USA; 2011.
[12] Snider DM. An Incompressible Three-Dimensional Multiphase Particle-in-Cell Model for Dense Particle Flows. Journal of Computational Physics. 2001;170(2):523-49.
[13] Cloete S, Amini S, Johansen ST. A fine resolution parametric study on the numerical simulation of gas-solid flows in a periodic riser section. Powder Technology. 2011;205(1-3):103-11.
[14] Wen CY, Yu YH. Mechanics of Fluidization. Chemical Engineering Progress Symposium Series. 1966;62:100-11.
[15] Cloete S, Amini S, Johansen ST. On the Effect of Cluster Resolution in Riser Flows on Momentum and Reaction Kinetic Interaction. Powder Technology. 2011;In press.